Real-time Industrial Vision System for Automatic Product Surface Inspection

Zhe Cui, Wenkai Lu and Jinlin Liu
State Key Laboratory of Intelligent Technology and Systems, Tsinghua National Laboratory for Information Science and Technology, Department of Automation,
Tsinghua University, Beijing, China
Tel:+86-010-62788078 Country Code: 100084
Email: phy_cuiz10@163.com

ABSTRACT
Product surface inspection plays a significant role in industrial aspects. Large industrial manufacturing requires such inspection procedure of high speed and accuracy at a fairly reasonable cost, which is precisely the demand automatic surface inspection systems are applied to meet. In this paper, we have constructed a vision system prototype employing image processing and pattern recognition approaches to classify those defective products automatically. Our algorithm first collects products images, then send them to preprocess. After that, we implement pattern extraction based on Fourier-Mellin transform, and classify the product patterns based on principle component analysis as well as support vector regression. The prototype has proven itself reliable through reaching accuracy of more than 90%.

CCS Concepts
• Computer systems organization→Real-time systems→Real-time system architecture

Keywords
"industrial vision; surface inspection; image processing; pattern recognition"

1. INTRODUCTION
Product quality inspection is an essential part in industrial manufacturing. And the development of computer vision system has challenged traditional manual inspection by faster speed and lower cost [1]. The application of automatic inspection has shown efficient usages in true aspects such as food quality [2], tablets inspection [3], iron industry [4], textile fabric inspection [5], bridge cracks detection [6]etc.

The desperate demand of automatic surface inspection leads to a number of related researches. Aluze et al. conducted defect detection on specular surfaces by synthesizing images from up to thirty different illumination conditions [7]. This lighting technique has also been applied on 3-D surface quality control of cars' body [8]. Perng et al. developed a CRT panel inspection system through scratch enhancement and Blob Analysis [9]. Salis et al. designed an automotive inspection system for highly reflective surfaces, which used structured lighting to get high contrast images [10]. Adamo et al. built an inspection system prototype for stain glass examination by identifying scratch-like and spot-like defects [11]. Zhang et al. proposed a surface inspection system for metal, which combined wavelet transform and multi-class support vector machine (SVM) to distinguish several kinds of metal defects [12]. Mart ínez et al. built an inspection system for transparent products through specific lighting and adaptive threshold segmentation [13]. Možina et al. presented an automatic pharmaceutical tablets inspection system using the statistical appearance method [3]. V élez-Rivera et al. applied industrial vision to mangoes ripeness judgment using principle component analysis (PCA) [2]. Giuseppe Di Leo et al. built an online system inspecting copper coils by automatically measuring sizes of products [14]. Chen et al. used Scalar Invariant Feature Transform (SIFT) in automatic vehicle detection with unmanned aerial vehicles (UAVs) [15].

Although industrial vision system has been proven capable for defects inspection ,it has also met challenges in sophisticated real demands. The inspection algorithm is severely constrained by operation environment and target objects [16], which leads to the lack of generality. A reasonable approach to solving this problem is the systematic consideration. The algorithm should be general-purpose, and be robust on different objects and missions [17][18].

In this study, we propose a fast and robust industrial vision system for surface inspection. Our algorithm is inspired by the study of image registration, where polar Fourier transform is applied in frequency domain to estimate translation and rotation of an image [19]. First, We use traditional image processing techniques as preprocessing. Then we apply our pseudo-polar transform based method to execute pattern extraction step. After that, pattern recognition techniques using principle component analysis (PCA) and support vector regression (SVR) are employed to generate a label of the examined object. We have built an inspection system porotype which uses the proposed method to automatically classify products. We test our system on training and testing data sets, and the results show that the proposed method are capable for real industrial demand.

2. ARCHITECTURES AND METHODS
In this section, we present three major parts of our inspection system. In the first subsection, we introduce the general structure of our surface inspection system Subsection II presents the pattern extraction method using our proposed pseudo-polar transform method. Subsection III describes the application of machine learning algorithm of PCA and SVR for industrial product mark.

ICIME 2016, November 02-05, 2016, Istanbul, Turkey
© 2016 ACM. ISBN 978-1-4503-4761-7/16/11…$15.00
DOI: http://dx.doi.org/10.1145/3012258.3012276

The text should be in two 8.45 cm (3.33") columns with a .83 cm (.33") gutter.

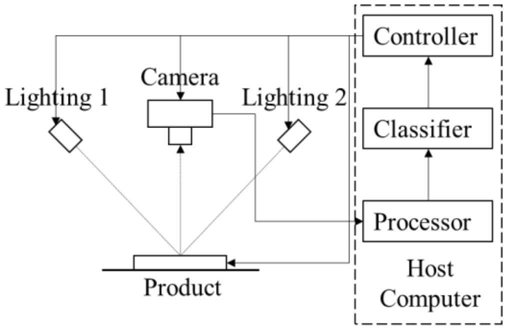

Figure 1. Inspection system architecture

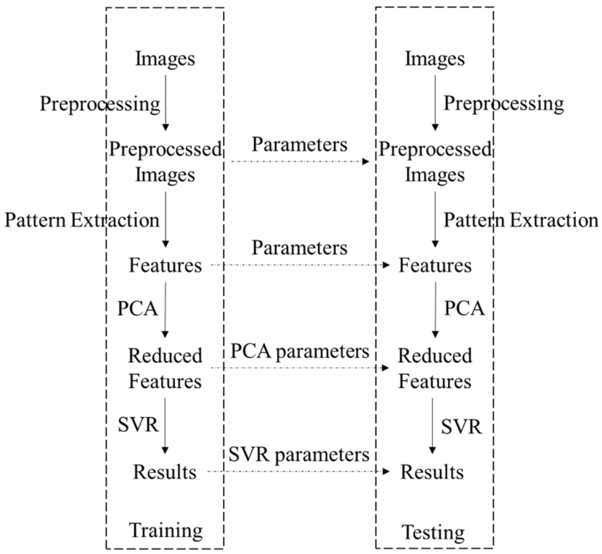

Figure 2. Framework of the production inspection system.

2.1 Inspection system architecture

A brief architecture of our system is shown in Figure 1. The system consists of two main components. First is a manufacture system, which assembles lighting equipment, camera and deliver belt for products. Second is a processing part in host computer, including steps of controlling equipment, image processing, and decision-making.

The product to be examined is delivered into the system by conveyor belt. Then the controller sends a signal to the lighting equipment and camera to take two photos of a product under low and high lighting conditions respectively. After that, the two photos are sent to the processor, where image processing and pattern extraction are employed to generate features. Next, according to the features obtained from the photos above, the classifier is able to judge whether the product is good or defective. Finally, the controller can identify the defective ones accurately, and moves them away.

As shown in Figure 2, in order to be easily manipulated, the processor and classifier on host computer are designed only to classify the images of products. The training of pattern classification is conducted on other devices by developers, which is to say, the training and running process are separated. All the manufacture workers need to do is to follow the abovementioned processes to operate the system.

2.2 Pattern extraction algorithm

In image registration studies, polar Fourier transform ,or Fourier-Mellin transform (FMT), has been employed to solve estimations of matching parameters [19-21]. Let I_2 be a translated and rotated copy of I_1:

$$I_2(x,y) = I_1\left(\left[x,y\right]\begin{bmatrix}\cos\theta & -\sin\theta \\ \sin\theta & \cos\theta\end{bmatrix} + \left[\Delta x, \Delta y\right]\right) \quad (1)$$

Where θ is the rotation angle, and $\left[\Delta x, \Delta y\right]$ is the translation parameter. Applying Fourier transform of Equation 1, and we can get:

$$F_2(u,v) = e^{-2\pi j(u\Delta x + v\Delta y)} F_1\left(\left[u,v\right]\begin{bmatrix}\cos\theta & -\sin\theta \\ \sin\theta & \cos\theta\end{bmatrix}\right) \quad (2)$$

It is easy to see that that magnitudes of spectra F_1 and F_2 are the same. But F_2 rotates an angle of θ counter clockwise. We can rewrite Equation 2 in a more simplified form using polar coordinates:

$$M_2(r,\varphi) = M_1\left(r, \varphi + \theta\right) \quad (3)$$

Where M_1 and M_2 are the magnitudes of Fourier spectra F_1 and F_2. Images from camera have locations shifted in that the products are on a moving conveyor belt. Therefore, the application of FMT neglects these shifts, and makes pattern extraction independent of locations.

Transforming Cartesian coordinates $\left[x,y\right]$ into polar coordinates $\left[r,\varphi\right]$ requires interpolation of gird, which leads to high computational cost. In our pseudo-polar method, we first set a polar grid of M angles and N radiuses, then separate pixels into this grid instead of interpolation directly. We sum all pixels' values in a single block of gird as a component of feature. Thus, a feature vector of $M \times N$ components is generated.

2.3 Machine learning algorithm

After previous pattern extraction steps, the algorithm generates features of K samples, and each sample has dimensions of $M \times N$. Before moving on to a classifier, principle component analysis (PCA) is applied to reduce dimensionality [22]. Let $X \in R^{K \times MN}$ be the data matrix, where each row of X represents a sample of feature dimension $M \times N$. PCA computes a subspace of dimension $L(L < K)$, and projects data X onto this space.

$$Y = XA \quad (4)$$

The new feature matrix Y and its corresponding labels are sent into a SVR classifier for training. The reason why we employ SVR rather than SVM is that the false negative rate (FNR) in SVR's result can be adjusted easier compared to SVM. In industrial inspection, false negative is more intolerable than false positive. It is required that products classified into "good" should not be inferior ones.

假阴性：被诊断为阴性（没病/良好）的人，实际患病。
此处即：被诊断为好的工件实际是有缺陷的工件。

At the same time, SVR classifier's outputs are float numbers, and the outputs' exact values depend on what we feed. Usually, we feed the inputs with -1 or $+1$, where -1 represents "bad" and $+1$ represents "good" [23]. And after training, SVR's result generally ranges in interval $[-1,+1]$. A threshold is set, upon which products will be labelled as "good", otherwise will be "bad". This threshold is adjusted by workers according to inspection results. If false negative rate increases, we lower the threshold value more along -1 direction so that more products are examined as "good". If false positive rate increases, we do the opposite.

3. EXPERIMENT RESULTS

To study the influence of parameters, we apply the abovementioned method in several experiments. The training data contains 198 good products and 105 defective products. Each product is photographed twice with different light exposure. All data and parameters are sent into the training program to generate those key parameters for testing. Data for testing contains 128 good and 88 bad products. Figure 3 displays original photos as well as ones after pre-processing, which are taken under different light conditions. As we can see, products are separated from the background operating machine properly.

There exists a bunch of parameters that can affect classification results. However, the subspace dimension L in PCA and kernel size σ in SVR classifier are the two most crucial parameters. We mainly discuss these two parameters, and their influences on training and testing results are illustrated in Figure 4.

Figure 4(a) presents the training and testing error over different PCA subspace dimension L, where other parameters stay constant. Obviously, both training and testing error rates drop as L increases. It simply infers that a larger L uses more information from original data, and has larger accuracy. Figure 4(b) shows the influence of kernel parameter σ, where larger σ means the classifier is smoother. As σ decreases, training error rate drops, until it reaches zero. While if σ falls too rapidly, the testing error rate will increase. In other words, the classifier is so twisted that it overfits on training data.

Meanwhile, figure 4(c) suggests that using two pictures improves little than only one. To put it another way, the picture taken on low exposure plays a key role. After checking the raw data, we find out that all labels whether a product is good or bad are manually done by experienced workers. However, they just check products on regular light condition, which is in the low exposure situation. Figure 5 displays two photos of a good product. Under low exposure, it seems all right in 5(a). But in 5(b), it looks like defective under high exposure. Therefore, it leads to the fact that only one photo's content is used.

Figure 4(d) also shows the receiver operating characteristic (ROC) curve of our classifier using default parameter. By adjusting the SVR threshold, we can get different pairs of false positive rate (FPR) as well as true positive rate (TPR). And the result of ROC curve proves that our classifier gives a better classification result for surface inspection, which proves the practicability of our method.

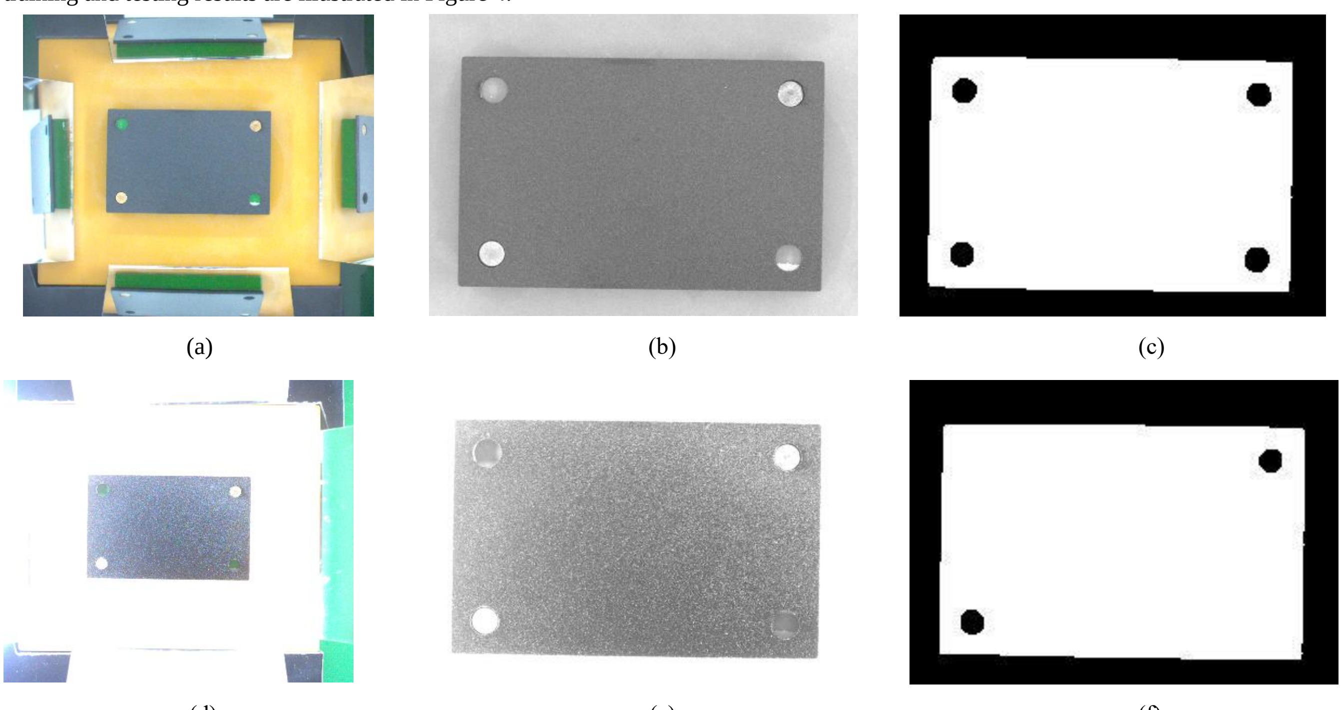

Figure.3 Photos and pre-processing results of a product. (a): Image under low exposure. (b): Selected region of (a). (c): Threshold separation of (b). (d): Image under low exposure. (e): Selected region of (d). (f): Threshold separation of (e).

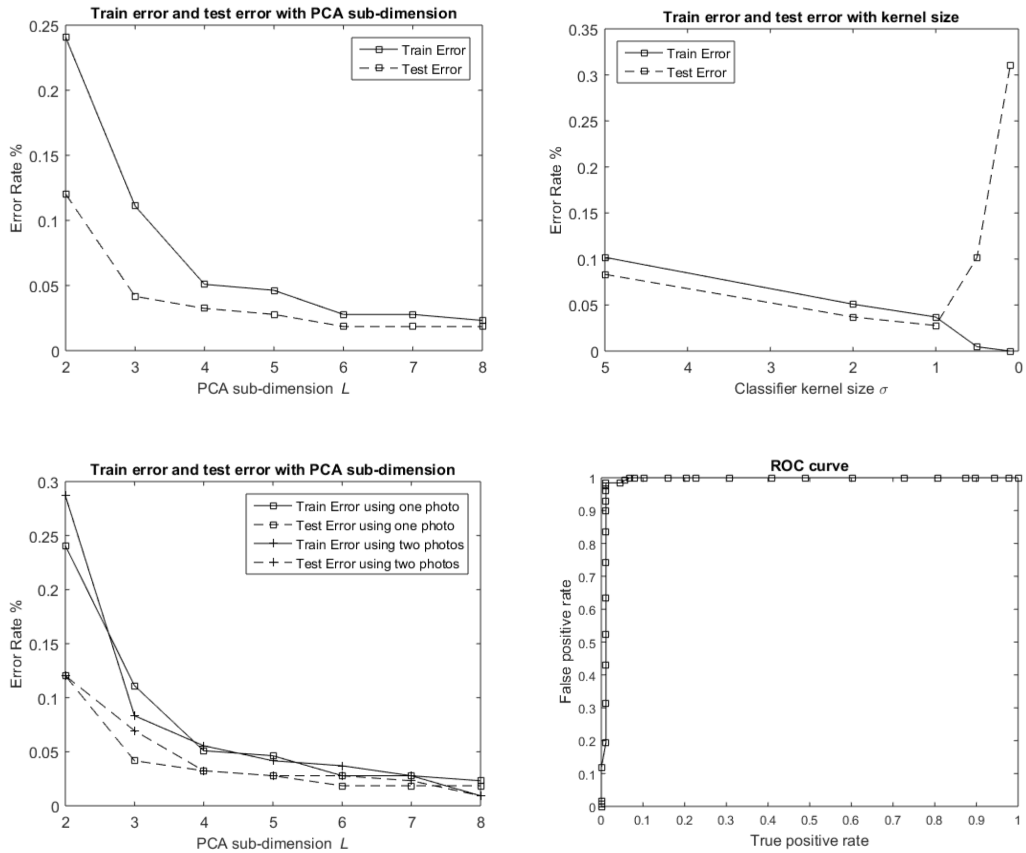

Figure 4. (a): Train error rate and test error rate as L changes; both two images with different exposure are used. (b): Train error rate and test error rate as σ changes; both two images with different exposure are used. (c): Train error rate and test error rate as σ changes; situations using one photo and two photos are compared. (d): ROC curve with default parameters.

4. FIGURES/CAPTIONS

We have constructed a novel method for automatic product classification through image processing and machine learning algorithm. The method extracts patterns from good and defective samples, and trains a classifier to separate them. The training and testing devices are independent so that the testing part can be easily manipulated by industrial workers. The proposed method has proven valid on real industrial manufacturing, and can distinct those defective products as expected.

5. REFERENCES

[1] T.S.Newman and A.K. Jain, A survey of automated visual inspection. Computer Vision and Image Understanding, (1995). **61**(2): p. 231-262.

[2] N. Velez-Rivera et al., Computer Vision System Applied to Classification of "Manila" Mangoes During Ripening Process. Food and Bioprocess Technology, (2014). **7**(4): p. 1183-1194.

[3] M. Možina et al., Automated visual inspection of imprint quality of pharmaceutical tablets. Machine Vision and Applications, (2013). **24**(1): p. 63-73.

[4] M.J. Thurley and T. Andersson, An industrial 3D vision system for size measurement of iron ore green pellets using morphological image segmentation. Minerals Engineering, (2008).

[5] R. Stojanovic et al., Real-Time Vision-Based System for Textile Fabric Inspection. Real-Time Imaging, (2001). **7**(6): p. 507-518.

[6] Y. Yeboah et al., Robotic Crack Detection and Classification via AdaBoost-RVM Implementation. International Journal of Mechanical Engineering and Robotics Research, 2015. 4(4): p. 361-367.

[7] D. Aluze et al., Vision system for defect imaging, detection, and characterization on a specular surface of a 3D object. Image and Vision Computing, (2002). **20**(8): p. 569-580.

[8] J. Leopold, H. Gunther and R. Leopold, New developments in fast 3D-surface quality control. MEASUREMENT, (2003). **33**: p. 179-187.

[9] P. Der-Baau, C. Cheng-Chuan and C. Wei-Yu, A novel vision system for CRT panel auto-inspection. Journal of the Chinese Institute of Industrial Engineers, (2007). **24**(5): p. 341-350.

[10] R. Seulin, O. Morel and F. Meriaudeau, Machine vision system for the inspection of reflective parts in the automotive industry, in Proc. SPIE, (2007).

[11] F. Adamo et al., An online defects inspection system for satin glass based on machine vision, in 2009 IEEE Intrumentation and Measurement Technology Conference. (2009): p. 288-293.

[12] Z. Xue-wu et al., A vision inspection system for the surface defects of strongly reflected metal based on multi-class SVM. Expert Systems with Applications, (2011). **38**(5): p. 5930-5939.

[13] S.S. Mart ńez et al., An industrial vision system for surface quality inspection of transparent parts. The International Journal of Advanced Manufacturing Technology, (2013). **68**(5-8): p. 1123-1136.

[14] G. DiLeo et al., A vision system for the online quality monitoring of industrial manufacturing. Optics and Lasers in Engineering, (2016).

[15] X. Chen and Q. Meng, Self-Learning Vehicle Detection and Tracking from UAVs. International Journal of Mechanical Engineering and Robotics Research, 2016. 5(2): p. 149-155.

[16] T.C. Henderson, Efficient 3-D object representations for industrial vision systems. IEEE Transactions on Pattern Analysis and Machine Intelligence, (1983). **5**(6): p. 609-618.

[17] H. Golnabi and A. Asadpour, Design and application of industrial machine vision systems. Robotics and Computer-Integrated Manufacturing, (2007). **23**(6): p. 630-637.

[18] E.N. Malamas et al., A survey on industrial vision systems, applications and tools. Image and Vision Computing, (2003). **21**: p. 171-188.

[19] Y. Keller, A. Averbuch and M. Israeli, Pseudopolar-based estimation of large translations, rotations, and scalings in images. IEEE Transactions on Image Processing, (2005). **14**(1): p. 12-22.

[20] B.S. Reddy, and B.N. Chatterji, An FFT-based technique for translation, rotation, and scale-invariant image registration. IEEE Transactions on Image Processing, (1996). **5**(8): p. 1266-1271.

[21] G. Tzimiropoulos et al., Robust FFT-Based Scale-Invariant Image Registration with Image Gradients. IEEE Transactions on Pattern Analysis and Machine Intelligence, (2010). **32**(10): p. 1899-1906.

[22] S. Wold, K. Eebensen and P. Geladi, Principal component analysis. Chemometrics and Intelligent Laboratory Systems, 1987. 2(1-3): p. 37-52.

[23] M. Awad and R. Khanna, Support Vector Regression. Neural Information Processing – Letters and Reviews, 2007. 11(10): p. 203—224.